Review Article

Roberto Caputo, Antonio De Luca, Giuseppe Strangi, Roberto Bartolino, Cesare Umeton*, Luciano De Sio, Alessandro Veltri, Svetlana Serak and Nelson Tabiryan

The POLICRYPS liquid-crystalline structure for optical applications

https://doi.org/10.1515/aot-2018-0027
Received May 24, 2018; accepted August 15, 2018; previously published online September 27, 2018

Abstract: We present a review of polymer-liquid crystal-based devices for optical applications. Starting from a particular fabrication technique, which enables to obtain the POLICRYPS (POlymer LIquid CRYstal Polymer Slices) structure, we illustrate different realizations, along with their working principle and main features and performances. The name POLICRYPS indicates a structure made of parallel slices of pure polymeric material alternated to films of well-aligned nematic liquid crystal (NLC), with a spatial periodicity that can be settled in the range $0.2 \div 15$ μm. Suitably designed samples can be utilized as optical devices with a high efficiency, which can be switched on and off both by applying an electric field of a few V/μm or by irradiating samples with a suitable light beam. In different geometries, POLICRYPS can be specialized to operate as switchable diffraction grating, switchable optical phase modulator, switchable beam splitter, or tunable Bragg filter. The POLICRYPS framework can be also used as a soft matter template for aligning different types of LCs or to create an array of tunable microlasers. Finally, we present a POLICRYPS structure with a polar symmetry of the director alignment, which enables local shaping of light polarization, allowing to convert circularly polarized beams into cylindrical vector beams.

Keywords: Bragg filter; diffraction grating; electro-optical device; liquid crystals; POLICRYPS.

***Corresponding author: Cesare Umeton,** CNR-Nanotec, UOS Cosenza, Dipartimento di Fisica, Università della Calabria, Cubo 31C, Ponte Pietro Bucci, 87036 Rende, Italy, e-mail: cesare.umeton@fis.unical.it
Roberto Caputo, Antonio De Luca and Roberto Bartolino: CNR-Nanotec, UOS Cosenza, Dipartimento di Fisica, Università della Calabria, Cubo 31C, Ponte Pietro Bucci, 87036 Rende, Italy
Giuseppe Strangi: Department of Physics, Case Western Reserve University, Cleveland, OH, USA
Luciano De Sio: Department of Medico-Surgical Sciences and Biotecnologies, Sapienza Università di Roma, Piazzale Aldo Moro, 5, 00185 Roma RM, Italy
Alessandro Veltri: Colegio de Ciencias e Ingeniera, Universidad San Francisco de Quito, Quito, Ecuador
Svetlana Serak and Nelson Tabiryan: Beam Engineering for Advanced Measurements Company, Orlando, FL, USA

1 The POLICRYPS structure

Great attention has been recently devoted to the investigation of switchable holographic structures based on holographic polymer-dispersed liquid crystals (HPDLCs), which means droplets of nematic liquid crystals (NLCs) dispersed in a polymer matrix [1, 2]. In fabricated samples, the average size of the NLC droplets is, in general, comparable to the wavelength of the impinging light, a circumstance that causes a strong scattering, thus, limiting the application-oriented utilization of these structures. For this reason, we designed and investigated a new kind of holographic grating called POLICRYPS (acronym of POlymer LIquid CRYstal Polymer Slices), which is made of slices of almost pure polymer alternated to films of uniformly aligned NLCs. Samples, which present a sharp morphology and a high optical quality, with low scattering losses, are realized by means of the holographic optical setup shown in Figure 1. This exploits an active stabilization system for the suppression of the vibrations that the sample might undergo during the curing process [3]. The standard fabrication procedure exploits the high diffusivity of LC molecules in the isotropic state to avoid the formation of the nematic phase during the curing process [4, 5]. In other words, during the fabrication procedure, by heating up the sample at a temperature value higher than the nematic-isotropic point of the LC medium, a high diffusivity of the LC molecules in the isotropic phase is enabled, which results in their almost complete separation from the polymeric ones. The physico-chemical mechanisms taking place during this high-temperature curing result in the formation of polymeric walls alternated to films of LC molecules in the isotropic phase. When this process comes to an end, the sample

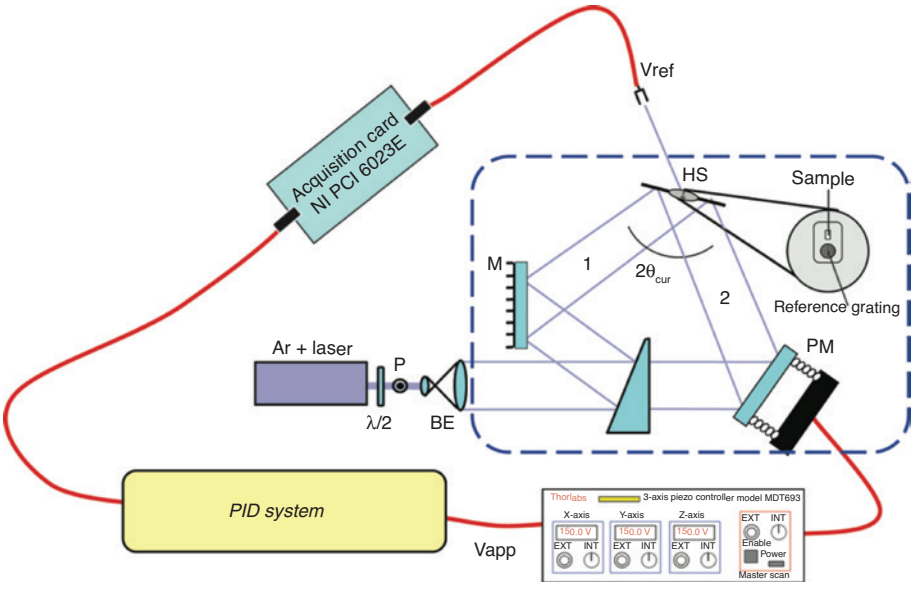

Figure 1: Optical holographic setup for UV curing gratings with stability check.
P, polarizer; λ/2, half-wave plate; BE, beam expander; BS, beam splitter; 2θcur, total curing angle; M, mirrors; S, sample; PD_1, first beam photodetector; PD_2, second beam photodetector; PD_3, diffracted and reflected beam photodetector. Inset: reference grating (positioned immediately below the sample area) that enables the stability check. Reprinted with permission from Ref [3], Optical Society of America (with full citation in reference list).

is slowly cooled down to room temperature to allow the LC molecules to self-assemble in a well-ordered and uniformly aligned nematic phase; as a result, the realized POLICRYPS sample is made of polymeric slices alternated to films of well-aligned NLCs.

The main fabrication steps are the following. A cell containing a homogeneous mixture of NLC, monomer, and photo-initiator is placed in a hot stage and heated above the nematic-isotropic transition temperature of the NLC component; in this condition, the sample is ready to be 'cured'. The light beam from an Ar-ion laser ($\lambda_B = 0.351\ \mu m$) is broadened up to a diameter of about 25 mm by a beam expander and divided into two parts of almost equal intensity by a beam splitter. The two beams overlap at the entrance plane of the sample cell and produce an interference pattern, which is used to cure the monomer of the mixture; the spatial period of this pattern can be easily settled in the range $\Lambda = 0.2 \div 15\ \mu m$, by adjusting the interference angle between the two beams. The stabilization system can continuously compensate for the optical path length variations that can take place due to slow variations in environmental conditions; residual fluctuations are, in fact, of the order of 6–7 nm, which corresponds to the sensitivity of the used piezo system. When the curing process is completed, the sample is slowly cooled down below the isotropic-nematic transition point and is ready for use.

Lately, the initial 'single-step' POLICRYPS fabrication procedure was implemented in a new 'multi–step' procedure, which enables the possibility of putting any desired liquid material between the polymeric slices [6]. After the described standard procedure is completed using a low-quality NLC, an etching process of the sample is carried out by immerging it (without opening the cell) in a water solution of tetrahydrofuran (THF); in this way, the solvent washes out the NLC from the polymeric framework. In a few hours, this process, which takes place above the nematic-isotropic transition temperature of the NLC, removes it without affecting the regularity of the structure. In a third step, the channels can be filled with a new desired liquid material, which may include photo-responsive, cholesteric, or ferroelectric liquid crystals, for the desired application.

2 The POLICRYPS switchable diffraction grating

The first basic device realized using a POLICRYPS holographic structure is an electro/all optical switchable transmission grating; it can, in principle, completely diffract or transmit an impinging light beam, depending on the application of an external voltage or irradiation with a suitable light. To investigate the characteristics of the grating, the impinging intensity I_{in} of the probe beam and the transmitted intensity I_{tr} are measured before starting

the curing process. Once this process is completed, and the UV light is turned off, the intensity I_0 of the directly transmitted and the intensity I_1 of the first-order diffracted beam are detected. In this way, it is possible to evaluate the zero-order transmittivity $T_0 = I_0/I_{in}$, the first-order transmittivity $T_1 = I_1/I_{in}$, the total transmittivity $T_{tot} = T_0 + T_1$, and the first-order diffraction efficiency, which is usually calculated as $\eta_1 = I_1/(I_0 + I_1)$. During the experiment, the intensity of the probe beam is maintained at a low, fixed, value. In general, the first-order diffraction efficiency of the POLICRYPS grating, measured at room temperature, turns out to be $\eta_1 \geq 90\%$.

The electro-optical response of the grating is investigated by exploiting a low-frequency (500 Hz, square wave) voltage, which is applied to the indium tin oxide (ITO)-coated glasses of the cell. Consequently, an electric field is created through the bulk of the cell, and the NLC confined between the polymeric walls reorients along the E-field direction; this induces an increasing refractive index contrast between the polymer and the NLC. The results are reported in Figure 2. The behavior of the first-order transmittivity T_1 (circles), zero-order transmittivity T_0 (squares), and total transmittivity T_{tot} (triangles) is reported versus the applied electric field r.m.s. values. T_{tot} turns out to be only slightly lower than 1 and remains approximately the same for all the values of the applied field; this result represents a clear indication that the grating exhibits negligible scattering losses. As for the switching field values, the first diffracted beam is almost completely switched off by a field of about 4.3 V/μm, while rise and fall times are about 0.9 ms and 1.1 ms, respectively.

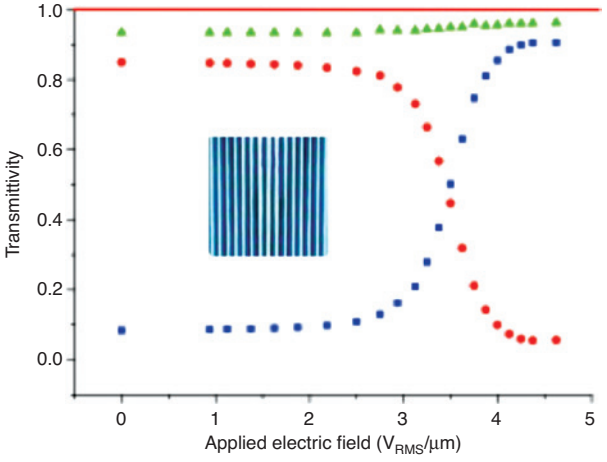

Figure 2: Dependence on an applied voltage of the zero-order transmittivity T_0 (squares), first-order transmittivity T_1 (circles), and total transmittivity T_{tot} (triangles) for a POLICRYPS grating. Picture in the inset shows a typical POLICRYPS grating morphology observed with a polarizing optical microscope. Reprinted with permission from Ref [4], Optical Society of America (with full citation in reference list).

The dependence of the diffraction efficiency η of a POLICRYPS grating on different physical and geometrical parameters can be interpreted in the framework of the Kogelnik model [7, 8], according to the following expression:

$$\eta = \sin^2\left(\frac{\pi(\varepsilon_1\varepsilon_{-1})^{1/2}L}{\sqrt{\varepsilon_0}\lambda\cos\beta}\right) = \sin^2(\psi(L, \lambda, T))$$

where λ is the vacuum wavelength of the probe radiation, L is the cell thickness, ε_i (i = 1, –1) stands for the i-th Fourier component of the dielectric constant distribution across the fringe, β is the refraction angle of the probe beam inside the sample, and T is the temperature. Therefore, η is an oscillating function of the argument ψ, with a periodical sequence of maxima and minima, which holds 1 and 0, respectively; ψ depends on the sample thickness, the probe wavelength and, following the ε_i dependence on temperature, is a monotonous decreasing function of temperature both for s and p polarizations of the probe wave. The small temperature dependence of the polymer dielectric constant can be, in general, neglected.

Recently, we realized optically switchable, high-quality POLICRYPS gratings by including, in the initial mixture utilized for its fabrication, a small concentration of azo-composite LCs, which are photo-responsive in the visible range (PLCs) [9, 10]. These are good materials for efficient all-optical switching applications due to their high photosensitivity to visible wavelengths, nanosecond response times, and fast relaxation [11]. By utilizing a LC in the multi-step fabrication process of the POLICRYPS framework, it is possible to realize an all-optical diffraction grating, controlled in the visible range that, in fact, represents a step forward in comparison to previously obtained results [12, 13]. The all-optical behavior of one of this kind of samples can be investigated by means of the setup shown in Figure 3A, which exploits a green diode laser (pump) emitting at λ = 532 nm (in the high absorption range of the mixture spectrum) and a He-Ne probe beam at λ = 633 nm; this beam impinges at the Bragg angle (11.5°) and is p-polarized, in order to experience the highest index contrast [13]. Figure 3B shows the typical change in the diffraction efficiency of an azo-LC-based POLICRYPS, induced by the pump green light. When the pump is switched on, the probe light experiences the average refractive index of the LC, whose value is close to the polymeric one, and a drop of the diffraction efficiency is observed. If the green pump beam is switched off, a cis-trans photoisomerization of the azo-based LC

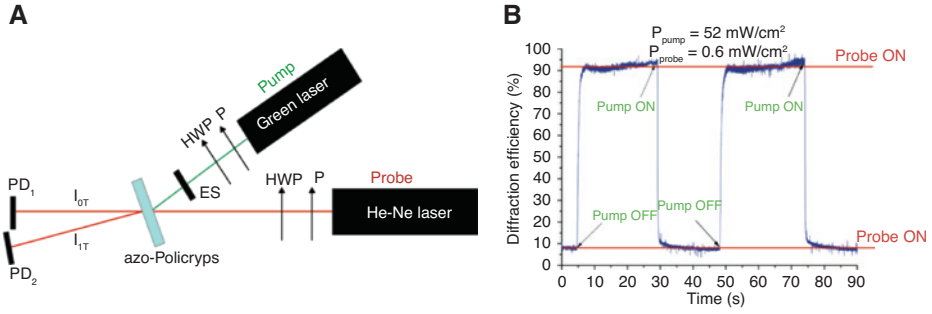

Figure 3: Experimental setup for the observation of all-optical processes in POLICRYPS diffraction gratings containing azo-LC. $PD_{1,2}$, photodetectors; HWP, half-wave plate; P, polarizer; ES, electronic shutter (A). Reversible and repeatable changes in the diffraction efficiency of the grating are induced by a pump green light. Power density values are indicated (B). Reproduced from L. De Sio, A. Veltri, C. Umeton, S. Serak, and N. Tabirian, Appl. Phys. Lett. 93, 181115 (2008), with the permission of AIP Publishing.

occurs, which induces reorientation of the LC director and restores the diffractive-index modulation of the sample. The switching behavior is detected by applying a periodic on-off pump beam irradiance sequence, while the intensity of the probe red beam is kept constant. The response of the grating turns out to be reversible and repeatable.

3 The POLICRYPS switchable optical phase modulator

The good morphology of the POLICRYPS structure enables using it as high quality, NLC-based, switchable phase modulator [14]. A basic device of this kind, already known in literature, uses a NLC with positive dielectric anisotropy that is contained in a cell whose glasses, previously treated to give a planar alignment to the NLC director, are coated with ITO films. The NLC birefringence yields a separation into ordinary and extraordinary waves of an impinging light beam (with wavelength λ) when it propagates through the structure. If L is the thickness of the sample and Δn the NLC birefringence, the phase difference ϕ between the two waves, measured at the exit of the sample, depends on the value of Δn according to $\phi = 2\pi L\Delta n/\lambda$. By means of the ITO films, an external electric field can be applied perpendicularly to the cell glass slabs, thus, reorienting the director **n** along the same direction of the field; this produces a change in the sample birefringence and, as a consequence, in the phase difference between ordinary and extraordinary waves. This basic device exhibits a great drawback in the great sensitivity to those temperature variations that are unavoidably induced by an impinging radiation of high power. The POLICRYPS structure can be used to avoid this problem, as the polymeric framework that confines the NLC molecules in films as tiny as few µm stabilizes their alignment. Furthermore, it turns out that the reorientation of **n** can be driven by low voltages, with short switching times [4]. Our test grating, with a periodicity $\Lambda = 1.22$ µm and a thickness $L = 6$ µm, is designed to exhibit a very low efficiency, thus, transmitting almost all the impinging light. The typical experimental setup for its fabrication is shown in Figure 4. The focalized light (spot diameter 0.5 mm, power density ≈ 1 mW/mm^2) from a He-Ne laser ($\lambda = 633$ nm) passes through a vertical polarizer before reaching the sample, placed in a rotation stage; this enables to set the POLICRYPS optical axis (given by the orientation of **n**) to any desired α angle with the polarization direction of the impinging light. Then, transmitted light passes through a second polarizer before reaching a photo-detector. As a reference signal, the transmitted intensity (zeroth diffracted order) I_{0T} is measured immediately after the sample when its optical axis is parallel to that of the first polarizer; then, the output intensities after the second polarizer are detected for different values of α,

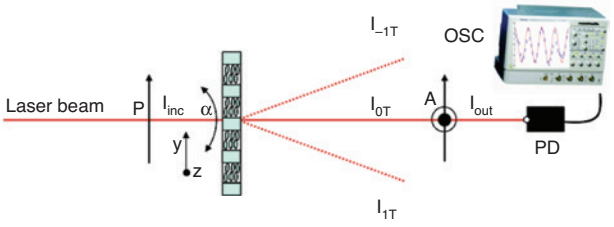

Figure 4: Experimental setup for utilization of the POLICRYPS as an optical phase modulator.
P, polarizer; A, analyzer; I_{inc}, total incidence intensity; I_{out}, output intensity, I_{0T} and I_{1T}, zeroth and the first-order transmitted intensities, respectively, α angle between the light polarization direction (y axis) and the grating axis (direction of the NLC director) in the *yz* plane; PD, photo-detector; OSC, oscilloscope. Reprinted with permission from Ref. [14], Optical Society of America (with full citation in reference list).

both between crossed (I_{cross}) and parallel ($I_{parallel}$) polarizers. The results in Figure 5A show that both intensities are periodic functions of the rotation angle α, a behavior that is typical of a retardation wave plate; the two curves for cross (I_{cross}) and parallel ($I_{parallel}$) intensities are drawn by starting from their minimum values. The results concerning the possibility of switching 'on' and 'off' the birefringence of the sample by applying an external electric field are shown in Figure 5B. The sample is placed between parallel polarizers, with its optical axis at 45° with respect to their axes. The applied field is increased from 0 V/μm to 7.1 V/μm; due to the director reorientation, the birefringence value is completely turned to zero. Finally, the stability of the device is demonstrated in Figure 5C, where its birefringence is reported versus the power of an impinging green (pump) laser beam (λ = 532nm). The very small observed variations indicate that the stabilization action of the POLICRYPS polymeric network noticeably reduces the thermal noise produced by the increasing impinging intensity [15].

The behavior of a POLICRYPS structure, operating as a phase retarder between a polarizer and an analyzer, is explained in the Jones matrix formalism [16, 17] (taking into account also the dichroic behavior of the structure), which gives the intensity I_{out} of the light transmitted by the analyzer as:

$$I_{out}(\beta) = \frac{I_{inc}}{2}[H^2 \sin^2\beta + V^2 \cos^2\beta + HV \sin 2\beta \cos\delta]$$

where I_{inc} is the impinging light intensity, β is the angle between the analyzer and polarizer axes, δ is the phase retardation (introduced by the plate) between the two orthogonal components $E_{||}$ and $E_{\perp}$ (with respect to the optical axis of the birefringent material), which the impinging wave is decomposed into. It can be evaluated from the expression [17]:

$$\cos\delta = \frac{1}{HV}\left[\frac{2I_{out}(\beta=\pi/4)}{I_{inc}} - \frac{H^2+V^2}{2}\right]$$

where parameters H and V depend on the considered material and can reflect a broad range of situations. They can be experimentally evaluated using the expressions:

$$H = \sqrt{\frac{2I_{out}\left(\beta=\pi/2\right)}{I_{inc}}};\ V = \sqrt{\frac{2I_{out}(\beta=0)}{I_{inc}}}$$

4 The POLICRYPS switchable beam splitter

The term optical beam splitter (OBS) indicates an optical device that splits an incident light beam into two or more beams. As an interesting way to obtain large area OBSs is to use periodic structures utilized in transmission mode, devices based on POLICRYPS or azo-POLICRYPS can be effectively exploited for OBS application. Furthermore, azo-POLICRYPS, when switched on and off [12, 13], can exhibit response times in the nanosecond range, a characteristic of particular interest for applications. We realized [18] an azo-POLICRYPS with L = 6.95 μm thickness and Λ = 1.57 μm fringe spacing: according to Kogelnik's theory [8], this grating operates in the Bragg regime, meaning that only one diffracted beam is observed. The experimental setup that enables using the azo-POLICRYPS as an optically controlled OBS is reported in Figure 6, along with the apparatus that produces an

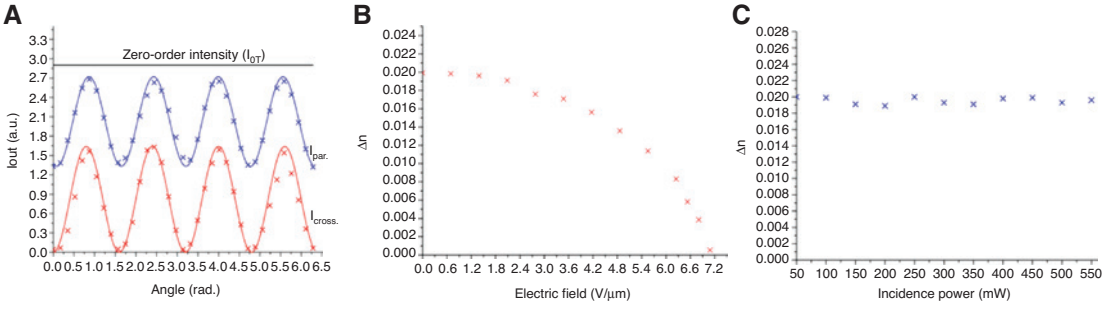

Figure 5: Output intensity detected versus the rotation angle α of the optical axis of the sample, placed between crossed (red) and parallel (blue) polarizers.
The difference between the level of I_{0T} and the maximum value reached by $I_{parallel}$ is due to the absorption of the second polarizer (A). Birefringence versus the applied electric field (square voltage pulses at 1 kHz) (B). Birefringence versus the power of the impinging laser beam (C). Reprinted with permission from Ref [14], Optical Society of America (with full citation in reference list).

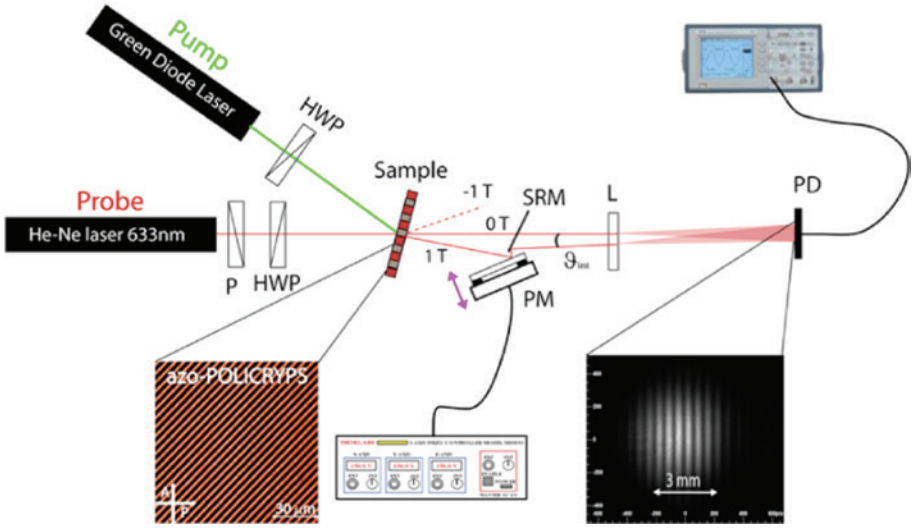

Figure 6: All-optical OBS and interferometer setup: P, polarizer; HWP, half-wave plate; SRM, semireflective mirror; θ_{int}, interference angle; PM, piezomirror; PD, photodetector; L, lens.
Reproduced from L. De Sio, A. Tedesco, N. Tabiryan, and C. Umeton, Appl. Phys. Lett. 97, 183507 (2010)], with the permission of AIP Publishing.

interference pattern with a tunable fringe visibility. The azo-POLICRYPS grating splits an impinging probe laser light ($\lambda = 633$ nm) into two beams (the transmitted and the diffracted orders, 0T and 1T, respectively), which are recombined in a Mach-Zehnder interferometer (needed to monitor the functionality of the OBS). The diffraction efficiency η of the grating is optically driven by an external pump beam (laser light at $\lambda = 532$ nm); Figure 7 shows η variations obtained by switching ON and OFF

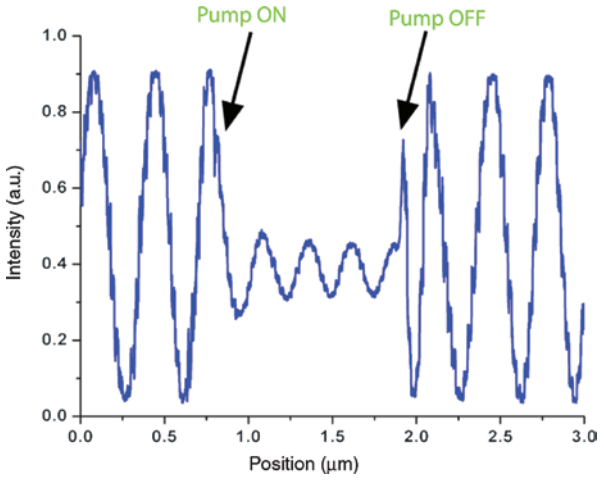

Figure 7: Intensity profile of the interference pattern versus the piezomirror position.
The reversible change in oscillation amplitude is obtained by switching on and off the external pump light. Reproduced from L. De Sio, A. Tedesco, N. Tabiryan, and C. Umeton, Appl. Phys. Lett. 97, 183507 (2010), with the permission of AIP Publishing.

the pump green light (intensity $I_{pump} = 48$ mW/cm^2), while the intensity of the probe beam is kept on at all times (intensity $I_{probe} = 0.55$ mW/cm^2). The ratio $R = I_{1T}/I_{0T}$ of the intensities of 1T and 0T beams is related to the diffraction efficiency (η) of the azo-POLICRYPS trough the equation $\eta = I_{1T}/(I_{0T} + I_{1T}) = R/(1+R)$; in the experiment, the polarization of the probe beam and its incident angle are adjusted [5] to obtain a maximum diffraction efficiency value $\eta_{max} \approx 50\%$ (that is to say, $R_{max} \approx 1$) when the pump beam is off. Characterization of the azo-POLICRYPS-based OBS is made using the interferometer shown in Figure 6. The interference pattern (reported in the dark inset of Figure 6, produced by overlapping 0T and 1T) exhibits a periodicity that can be adjusted by varying the small (≈0.04°) angle ϑ_{int}. It can be shown that the fringe visibility, defined as $V = (I_{max} - I_{min})/(I_{max} + I_{min})$, (where I_{max} and I_{min} are the measured maximum and minimum intensity values of the interference pattern) depends on R through the equation $V = [2(I_{0T}I_{1T})^{1/2}/(I_{0T} + I_{1T})]|\gamma| = [2(R)^{1/2}/(1+R)]|\gamma|$, where the degree of coherence γ of the two beams [19] is related to the difference Δl of the optical path lengths of the two beams and to the coherence length l_c of the probe laser beam (of the order of 10 cm in our case). As in the experiment Δl never exceeds a few μm, it is reasonable to assume that $|\gamma| = (1 - \Delta l/lc) \approx 1$, which yields $V = 2[\eta(1 - \eta)]^{1/2}$. As the efficiency η varies with the impinging pump power P_{pump}, the characteristics of the tunable OBS can be investigated by measuring the fringe visibility V for different values of P_{pump}. For each value, the measurement is made by moving (linearly in time) the piezo-mirror PM of the interferometer

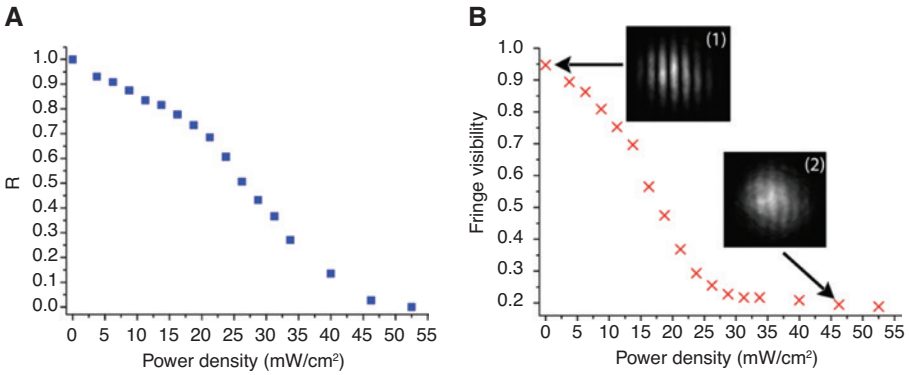

Figure 8: Beam splitting (A) and fringe visibility (B) are reported versus the pump power density.
The interference pattern acquired with a CCD camera is reported for $V = 0.94$ (inset 1) and $V = 0.2$ (inset 2). Reproduced from L. De Sio, A. Tedesco, N. Tabiryan, and C. Umeton, Appl. Phys. Lett. 97, 183507 (2010), with the permission of AIP Publishing.

of Figure 6, thus, varying the optical path length of one of its arms; this causes a scrolling of the fringe pattern on the photo-detector and enables the detection of both I_{max} and I_{min} values without shifting the PD from the center of the two interfering beams (of Gaussian shape). The behavior of V as a function of P_{pump} values is reported in Figure 8B, along with measured values of R in Figure 8A; this shows that R values can be finely adjusted between 1, which means that transmitted and diffracted beams have the same intensity, and 0, indicating that there is no diffracted beam, and the whole impinging intensity is transmitted.

As a final remark, where the temporal stability of the generated interference pattern is concerned, we have not observed any significant aging of the optical properties of the device in terms of contrast ratio and response times.

5 The POLICRYPS tunable Bragg filter

The POLICRYPS structure can be exploited to realize a tunable optical filter. Figure 9 shows a sketch of a device of this kind, based on a guided wave – POLICRYPS system [20]. A high index contrast ($\Delta n \cong 0.04$) channel, in-diffused, waveguide in BK7 glass substrate enables mono-modal propagation of light over the optical C-band (1530–1560 nm), with low propagation losses [21]. On top of the waveguide, a glass cover creates a gap, which is infiltrated with a mixture composed by UV-curable pre-polymer and common NLC. Then, using the standard UV curing process, a POLICRYPS grating is realized, which exhibits a spatial periodicity of about 2.5 μm and provides a Bragg wavelength of about 1550 nm for the fifth order of diffraction. Coplanar aluminum electrodes, patterned on

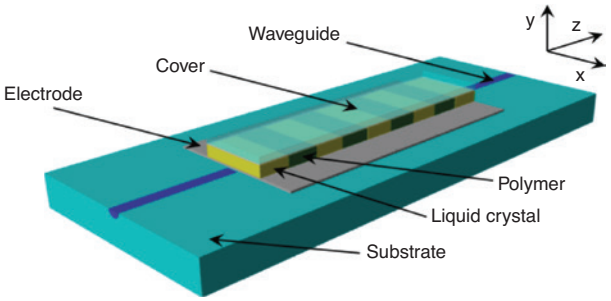

Figure 9: Sketch of an integrated optical filter including a POLICRYPS grating.

both sides of the channel waveguide, enable to apply an electric field. This is used to induce an in-plane director reorientation in the NLC contained in the POLICRYPS [20], which yields a variation of the refractive index modulation of the overlaying hybrid cladding; this can be experienced by a guided light wave with horizontal polarization (TE-like). Thus, application of an electric field to the device induces a tuning of the Bragg wavelength exhibited by the overlaying periodic structure, with a consequent tuning of the optical filtering effect in the guided wave.

The filter optical response of this device is carried out by exploiting an erbium-doped fiber amplifier (spectrum ranging from 1530 nm to 1565). An in-line fiber polarizer and a polarization controller ensure that only TE light enters the filter, which is fiber butt coupled at both the waveguide input and output. Optical transmitted and back-reflected spectra are analyzed by an optical spectrum analyzer. Figure 10A shows the detected transmission spectrum of the filter, whose bandwidth is related to grating parameters such as periodicity and effective refractive index, with a 20-dB suppressed signal at the Bragg wavelength of 1552 nm.

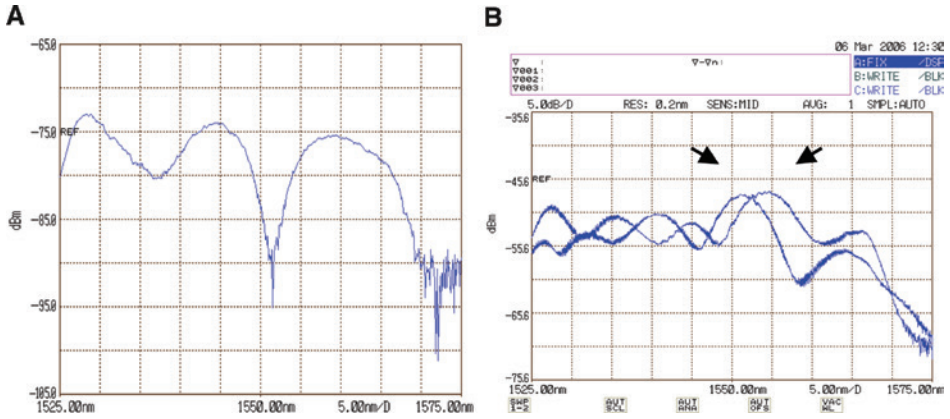

Figure 10: Transmitted (A) and tuned reflected (B) spectra of the POLICRYPS filter detected by an optical spectrum analyzer. Reprinted with permission from Ref. [20], Optical Society of America (with full citation in reference list).

An optical circulator introduced in the same setup enables detecting the filter-reflected spectrum. Figure 10B shows both the reflected spectra detected without any applied electric field and the one detected when applying a square-wave electric field (≈2.7 V/μm at 1 kHz) to the POLICRYPS structure. The filter exhibits a FWHM of ≈5 nm with a tuning range of ≈4 nm, which is driven by the amplitude of the electric field applied to the POLICRYPS.

An implementation of this device exploits an azo-POLICRYPS for realizing an integrated all-optical tunable filter, with all optical operations at the telecom wavelengths [21, 22]. A schematic and a micrograph of the filter are shown in Figure 11. The azo-POLICRYPS structure is

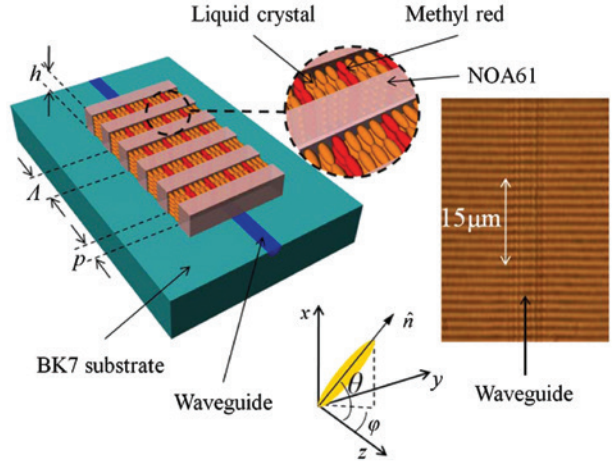

Figure 11: Schematic view of the device with a zoom on the grating structure.
The bottom inset sketches the orientation tilt (θ) and twist (φ) angles of the molecular director. The right micrograph shows the fabricated grating on top of the optical waveguide. Reprinted with permission from Ref [21], Optical Society of America (with full citation in reference list).

realized according to the multi-step procedure [6], using E7 NLC doped with methyl red (MR); the grating period is $\Lambda \approx 1.5$ μm. In the absence of a pump light, the MR molecules are in their elongated trans form, and both their long axis and the NLC director remain aligned perpendicularly to the polymer slices. In this way, the evanescent wave of a TE-like wave propagating in the waveguide experiences a phase grating in the overlaying POLICRYPS, due to the mismatch between the refractive index of the NOA61 ($n_p = 1.5419$ at $\lambda = 1550$ nm) and the one of the trans MR + E7 mixture ($n_\perp \approx 1.5$, for light polarization perpendicular to the LC director). Because of this grating, the device operates as a Bragg filter, with a back-reflected wavelength given by $\lambda_B = (2\Lambda n_{eff})/m$, where m is the diffraction order, and n_{eff} indicates the effective refractive index of the guided mode, which depends on the physical parameters of the structure; for $m = 3$, λ_B is in the range 1520–1570 nm (telecom). If the grating is irradiated by light at $\lambda = 532$ nm, the MR molecules turn in the spherical cis form, which strongly affects the directional order of the MR-E7 guest-host system: the mixture becomes optically isotropic with a refractive index whose average value

$$\langle n \rangle = \sqrt{\frac{n_{\parallel}^2 + 2n_{\perp}^2}{3}}$$

is estimated as $\langle n \rangle = 1.5655$ ($n_{\parallel} = 1.689$ and $n_{\perp} = 1.5$ [20]). This yields a variation in the mismatch with the polymer refractive index and a variation in the value of λ_B. Figure 12 shows the setup used to detect the transmitted spectra. An erbium-doped fiber amplifier is used as a broadband source operating from $\lambda = 1520$ nm to $\lambda = 1580$ nm; the filtered light is sent to an optical spectrum analyzer. The pump laser, emitting at $\lambda = 532$ nm, supplies a power $P \cong 45$ mW, which exceeds the trans-cis

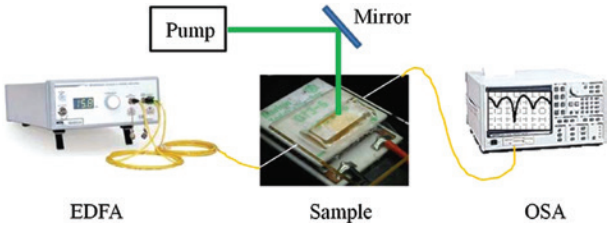

Figure 12: Setup used to detect the transmitted spectra of the tunable all-optical filter.
Reprinted with permission from Ref. [21], Optical Society of America (with full citation in reference list).

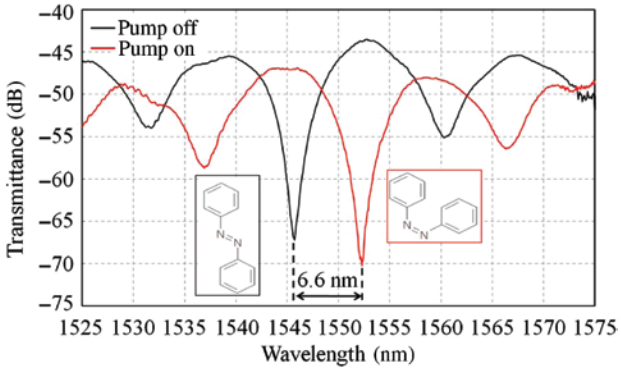

Figure 13: Transmittance of the all-optical filter.
Black line, pump off; inset with azo dye in trans phase; red line, pump on; inset with azo dye in cis form. Reprinted with permission from Ref. [21], Optical Society of America (with full citation in reference list).

transition threshold without affecting the temperature of the mixture. In Figure 13, the transmitted spectrum detected when the pump is off (black line) exhibits a notch peak of –20 dB at $\lambda_B = 1545.7$ nm. If the pump green light is turned on, the spectrum is shifted by 6.6 nm (red line), preserving its shape but with a slightly deeper notch of about –22 dB. The bandwidth of the transmitted notch, at –3 dB with respect to the transmittance minimum, is 3.3 nm with the pump off and 2.7 nm with the pump on. It is worth pointing out that measured results are in good agreement with predictions obtained using COMSOL Multiphysics as a simulation tool.

6 The POLICRYPS universal template for photonic applications

Single-step [4] and multi-step [6] POLICRYPS fabrication technology enables to fabricate a universal template that can be filled with active, soft-composite materials; then, LC alignment, chemical interactions, and confinement properties yield a self-organization mechanism that, exploiting the topology of the template, gives rise to advanced photonic properties. In particular, distinctive capabilities of the self-organization process are utilized with three different LC phases and mixtures to realize (i) a cholesterics-based system that exhibits particular optical activity features; (ii) chiral smectics-based system for ferroelectric fast switching, (iii) a dye-doped CLC-based system that works as a microlaser array.

(i) ULH configuration of cholesteric liquid crystals
Cholesteric liquid crystals (CLCs) are organized in layers with no positional order of molecules within each layer, but characterized by a director axis, whose orientation smoothly rotates from layer to layer; this director reorientation is helicoidal, with a pitch that can vary in the range 0.1–20 μm [23]. A further, in-plane rotation of the helical axis (the so called 'flexo-electric effect' [24]) is obtained by applying an electric field across the CLC film; at high temperature, the system exhibits a 'uniform lying helix' (ULH) configuration, in which the helical axis is uniformly aligned in the plane of the two confining substrates. A consequence of this flexo-electric effect is the so-called 'flexo-electro-optic effect' (FEO), which indicates an in-plane rotation of the optical axis of a short pitch CLC, aligned in a ULH texture, taking place under the action of an applied electric field [25]. We exploit our 'empty POLICRYPS template' to induce the ULH configuration of a short-pitch CLC. The template is filled with a CLC (BL088, helix pitch ~400 nm) at high temperature (~90°C), which keeps the CLC in the isotropic phase. When cooling down the sample to room temperature, a self-organization process occurs, which orients the CLC helices in the ULH geometry. Experimental features are investigated by utilizing a probe setup [26] and a sample, 10 μm in thickness, which maximize the light transmission [27]. Figure 14A shows a POM micrograph of the sample at the edge of the POLICRYPS template. On the left, the focal conic texture is due to a random distribution of the helical axes (high magnification in Figure 14C). On the right, the ULH geometry is induced by the structure (high magnification in Figure 14D). Electro-optical characterization of the area in Figure 14D is made by means of a voltage (1-kHz square wave, Figure 14B), applied across the cell, perpendicularly to the helix. The created electric field induces an in-plane tilt of the optical axis of the CLC, aligned in a ULH texture; the tilt is inverted if the direction of the electric field

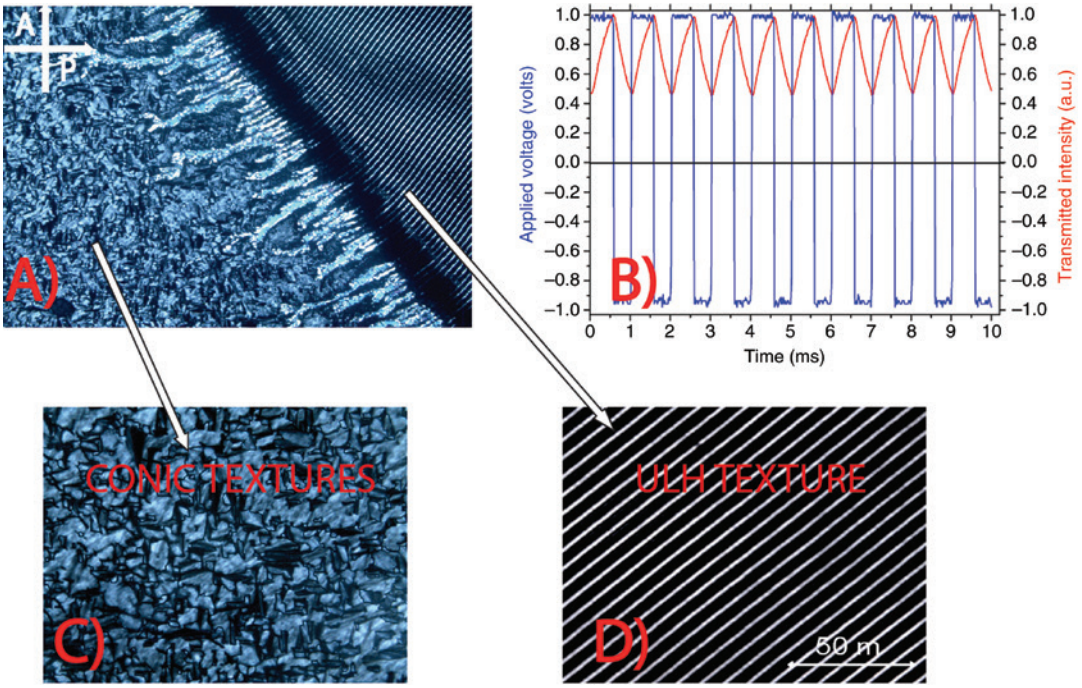

Figure 14: POM view of the template filled with short pitch CLC at the edge of the grating area (A). The high magnification of the random-oriented CLC area is reported in (C), while the CLC area aligned in ULH geometry is shown in (D); its electro-optical response is reported in (B). Reproduced with permission from Ref. [6]; copyright 2011, The Royal Society of Chemistry.

is reversed. The transmitted intensity (red curve in Figure 14B) is proportional to the electric field that induces the in-plane rotation of the sample optical axis [28].

(ii) Ferroelectric switching

Ferroelectric LCs (FLCs), exhibit a permanent polarization, without the action of any applied electric field [29] and are used to realize the so-called 'surface stabilized ferroelectric liquid crystal' (SSFLC) devices [30]. These can exhibit a fast response, a wide-view angle, and a bistable memory capability, but their overall optical performances are affected by mechanical stability and DC voltage balance [31]; thus, we explored the possibility to use POLICRYPS templates to align an FLC. This is injected into the template at a high temperature, above the LC clearing point (90°C); then, the sample is slowly cooled down to room temperature. The results, obtained with a cell thickness of $L = 10$ μm and a $\Lambda = 3$ μm pitch are satisfactory [6]. At the edge, the sample, observed with a POM, shows the focal conic texture of non-aligned FLC molecules (right view, Figure 15A, B); once realized, it behaves as a uniaxial plate (left view, Figure 15A, B). By rotating the sample 45° under the microscope, the SSFLC area (left) becomes dark, while the FLC region (right) remains almost unchanged; this is an experimental evidence that a director alignment occurs in the SSFLC region. In fact, the width of the POLICRYPS channels is of the same order of magnitude of the helical pitch and, due to boundary conditions, the molecular director is constrained at a given angle (22°) with the normal to the polymeric slices [32]. The electro-optical effect is obtained by applying a voltage that switches the director orientation (±22°). Consequently, the polarization axis (which is perpendicular to the molecular director) is switched between two stable states ('Clark-Lagerwall effect' [30]). Figure 15D shows the bistability of the SSFLC area (depicted in Figure 15C), measured using a bipolar electric pulse with a 1-ms period (blue curve, Figure 15D). The red curve in Figure 15D shows the two stable states of the transmitted intensity; jumps between them are driven by the applied bipolar voltage.

(iii) Microlaser array

A further application is represented by the realization of a POLICRYPS-CLC-based microlaser array. A CLC system behaves as a photonic band gap (PBG), i.e. due to a distributed feedback (DFB) mechanism, it exhibits a window in the electromagnetic spectrum where wave propagation is forbidden. Because of the DFB, the system behaves, in fact, as a mirrorless optical resonator, and if the CLC is doped with

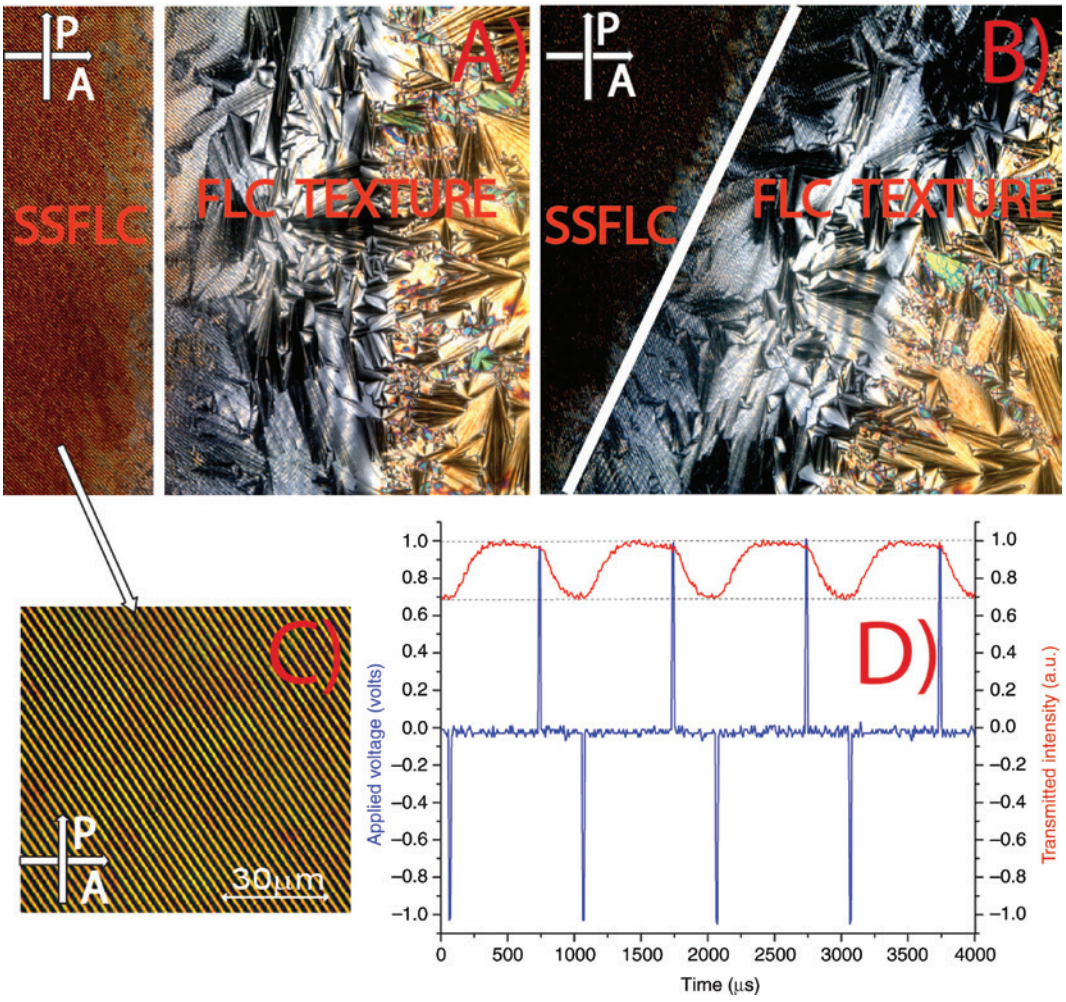

Figure 15: POM view of the template (grating vector aligned at 45° with the polarization direction) filled with short pitch FLC at the edge of the grating area (A) and after rotating the grating vector of 45° (B). The bistable electro-optical response of the depicted area (C) is reported in (D). Reproduced with permission from Ref. [6]; copyright 2011, The Royal Society of Chemistry.

fluorescent guest molecules, it is possible to obtain a gain enhancement of the radiation propagating in the structure [33, 34]. In standard CLC systems, the refractive index modulation is quite low, but in our case, the use of a POLICRYPS template as a framework for dye-doped CLC helices exhibits several advantages, as the single channel can be as long as several centimeters, thus containing thousands of periods of the CLC helices, a feature that enhances the DFB effect. In this way, each channel of the structure can behave as an optical resonator with a high-quality factor Q (also due to the small volume of the channel), suitable to make a microlaser. An array of parallel microlasers in a POLICRYPS structure is realized by adding a small amount of pyrromethene dye, representing the gain medium, to a mixture of CLC (BL088, Merck, Darmstadt, Germany) and monomer (NOA-61, Norland Products, Cranbury, NJ, USA), which includes also photoinitiators (Irgacure 2100 and Darocur 1173, Sigma Aldrich, Munich, Germany) [35]. The mixture, injected between two ITO-coated glass slabs, undergoes the classical 'single-step' procedure that yields a POLICRYPS [4]. Its channels, with a periodicity of about 5 μm and a width of about 1.5 μm), represent the laser microcavities that contain dye-doped CLC and are periodically separated by polymer slices. Microlasers are switched on when optically pumped with the second harmonic ($\lambda = 532$ nm) of a Nd:YAG pulsed laser, focused onto the sample and linearly polarized perpendicularly to the microcavities. The long axis (≈5 mm) of the elliptic laser spot section is oriented perpendicularly to the cavity orientation (Figure 16), thus ensuring the simultaneous excitation of multiple microlasers. Above a given threshold

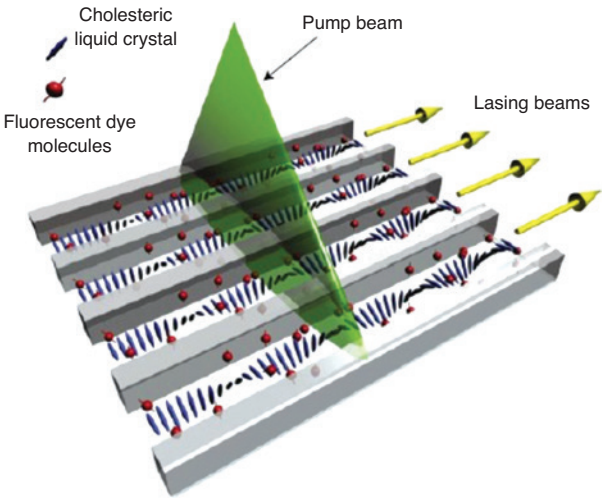

Figure 16: Sketch of a microlaser array realized in a POLICRYPS structure.

of the pump energy per pulse, light emission occurs, which emerges from the microcavities, along their direction and parallel to the glass plates. Light beams are circularly polarized, indicating that the DFB mechanism due to the CLC helices is the cause of the observed phenomenon. The lasing nature of this emitted light is demonstrated in Figure 17, where dependences on energy per pulse of the pump green laser are reported for emitted intensity and spectral linewidth (FWHM). At low excitation energies, both the emission intensity and the linewidth show an almost linear dependence on the pump energy. Above a characteristic threshold (≈25 nJ/pulse), the emitted intensity suddenly starts to increase very rapidly; in addition, above the same threshold value, the emission linewidth breaks off from the previous trend and begins to decrease significantly. Interestingly, the observed threshold in the pump energy value is one order of magnitude lower than in the cases of other conventional dye-doped systems in a similar environment and under the same pumping conditions. The spatial distribution of the laser emission is acquired, perpendicularly to the microchannels, by a high-sensitivity, high-resolution CCD camera that checks the near-field profile of the stimulated emission in the proximity of the output edge of the sample cell. The mapped intensity profile (Figure 18) indicates that the maxima of lasing intensities have a spatial recurrence, with a periodicity that is about 5 μm, in perfect agreement with the distance of polymeric slices in the POLICRYPS structure. Further experimental investigations demonstrated the possibility to tune the lasing wavelength by varying the sample temperature and to control the lasing intensity by applying an electric field, perpendicularly to the helical axis orientation. By varying the temperature from 25°C to 80°C, an average red-shift of 0.2 nm/°C is recorded in the spectral range 580–590 nm. As a matter of fact, indeed, the pitch of the CLC changes with temperature variations [36], thus, producing a shift of the stop band edge where the lasing is expected. On the other hand, by applying a sinusoidal voltage (1 kHz, from 0 up to 3.7 V/μm) to the sample between the two ITO-coated glass while maintaining fixed the pump energy, a significant decrease in the lasing intensity is observed;

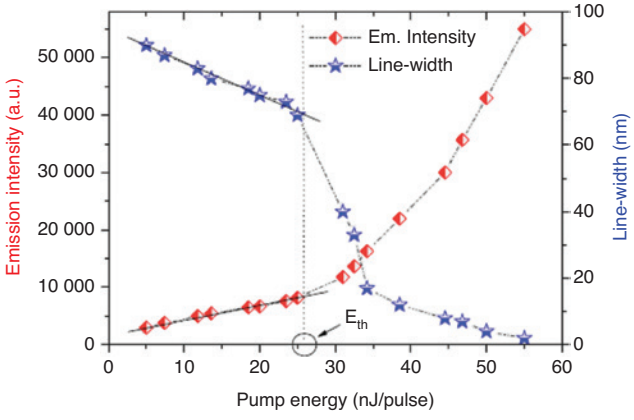

Figure 17: Emitted intensity and linewidth dependence on input pump energy.
Reproduced with permission from Ref. [35]; copyright 2005, The American Physical Society.

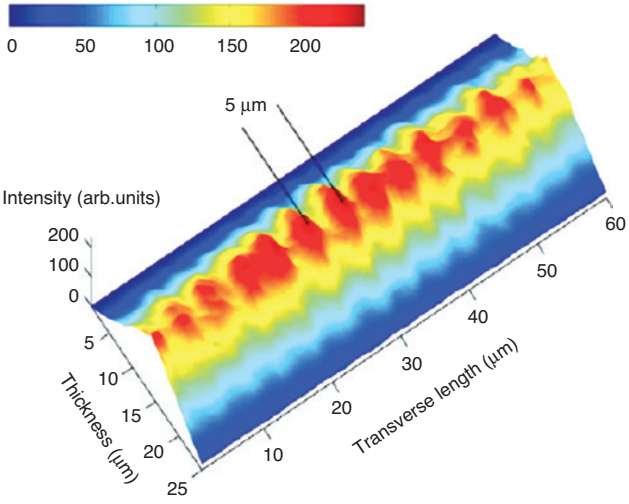

Figure 18: Spatial distribution of the laser emission emerging from the mirrorless microcavity laser array.
The periodicity of maximum intensities is 5 μm. Reproduced with permission from Ref. [35]; copyright 2005, The American Physical Society.

in addition, above a given field threshold, the micro-lasers switch off. This is because the electric field, applied perpendicularly to the helical axis, produces a local distortion of the CLC periodic structure, whose molecules tend to align along the electric field, thus modifying the sinusoidal modulation of the refractive index, which assumes a low-efficiency rectangular profile [37]. The overall result is a diminishing of the DFB mechanism; therefore, a decrease in the lasing intensity is observed. By further increasing the field, the regions where the molecules are favorably oriented (from the energetic point of view) keep expanding until the chiral helix completely unwinds, and the structure becomes nematic.

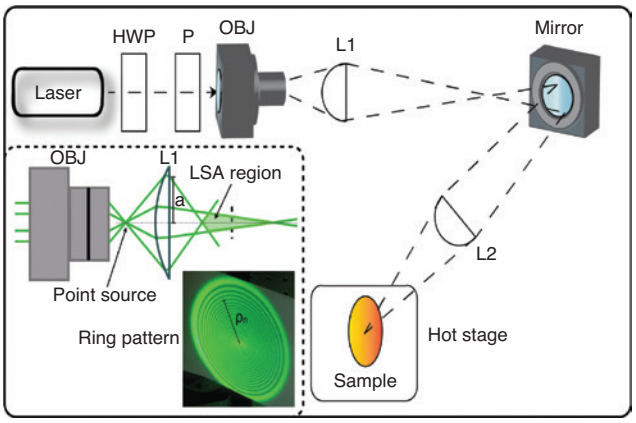

Figure 19: Optical setup for visible curing of polar POLICRYPS structure.
Laser, CW solid state laser; P, polarizing beam splitter; HWP, λ/2 plate; OBJ, microscope objective (10×); L_1, L_2, spherical lenses. The sample is put in a hot stage to accurately control its temperature. On the inset: sketch illustrating the spherical aberration the laser beam undergoes passing through the lens L_1 and the ring pattern imaged on a plane perpendicular to the optical axis of the system. Reprinted with permission from Ref. [39], Optical Society of America (with full citation in reference list).

7 The polar POLICRYPS structure for realization of q-plates

A planar slab of a uniaxial birefringent medium (like LC) can induce a homogeneous phase retardation of half-wave across the slab; in addition, an inhomogeneous orientation of the fast optical axis lying parallel to the slab planes can yield the consequence that the emerging wave not only is uniformly right-circular polarized but also acquired a phase factor $\exp(im\phi)$, i.e. it has been transformed into a 'helical' wave (the sample is a 'q-plate', with $m = 2q$) [38]. We have shown that, by properly shaping a POLICRYPS structure, it is possible to commute from a diffraction grating with a standard Cartesian geometry to a polar one of high-quality morphology [39], where an intrinsic radial orientation of LC director, obtained in all the rings of the sample, might enable the possibility of realizing optical q-plates. The fabrication of the circular POLICRYPS structure is performed by exploiting the setup reported in Figure 19. Power and polarization of the curing beam from a laser source ($\lambda = 532$ nm) are controlled by a half-wave plate (HWP) and a polarizing beam splitter (P). The beam is focused by a microscope objective (10×) to an almost point source of coherent light that, imaged by the lens L_1, experiences a spherical aberration. In the longitudinal spherical aberration image-space of the lens, a centro-symmetric diffraction pattern is produced, whose center is located on the optical axis of the system (Figure 19, inset). The produced pattern consists of very closely spaced concentric rings, whose spacing can range from a few micrometers to tens of micrometers, depending on the specific values of geometrical parameters. Because of spherical aberration, light rays coming from lens L_1 are not all focused on the same point, but rays passing through the lens in its extreme outer parts focus closest to the lens, while rays passing through the lens center focus at the most distant point from the lens; the region between these two focal points is called the longitudinal spherical aberration region (LSA). The obtained pattern, focused on the surface of the sample cell by means of lens L_2, is used to cure the photo-sensitive mixture, which is inside. The size of the obtained pattern is controlled by properly choosing the focus of L_2, while periodicity and number of rings are controlled by acting on the lens diameter, lens-to-source distance, and viewing conditions. Cells used for the realization of circular POLICRYPS are fabricated using two glass substrates to form a 10-μm cell filled with a photo-sensitive mixture made of the pre-polymer NOA61, the E7 NLC, and the photo-initiator Irgacure 784, which can be cured by exploiting visible-light curing in the framework of the standard POLICRYPS protocol [4]. Three samples with different numbers of rings and average pitch values ($\Lambda a \approx 100$ μm, $\Lambda b \approx 25$ μm, $\Lambda c \approx 5$ μm, see Figure 20) were realized by slightly modifying the setup in Figure 19, using optical elements (objective, lenses 1 and 2) with different magnifications and focal distances or by changing their relative distance. Micrographs of the obtained morphologies (taken between crossed polarizers at the polarized optical microscope) are shown in Figure 20. A whole view (Figure 20A) of the sample with the largest pitch ($\Lambda_a \approx 100$ μm) shows an evident Maltese cross that confirms the radial alignment of the LC component in all

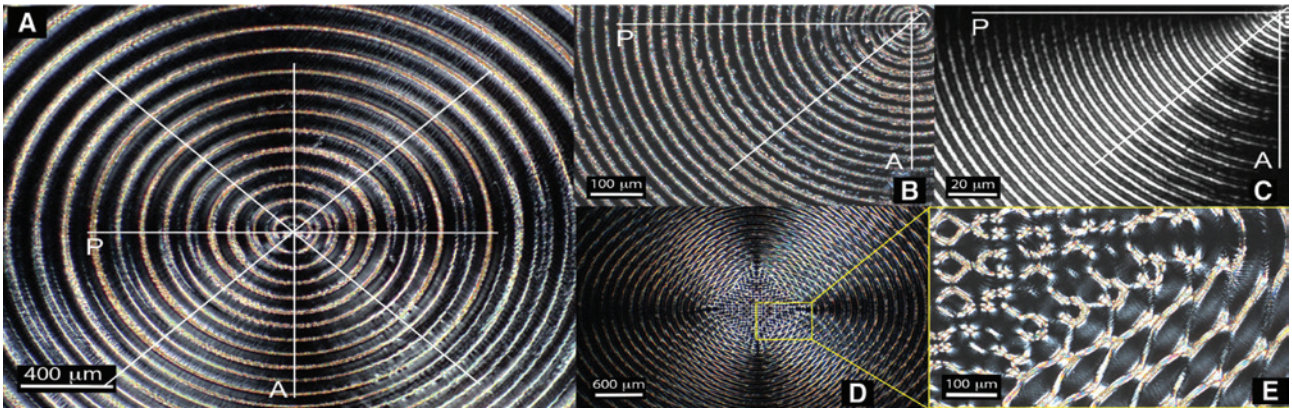

Figure 20: Micrographs (taken at the polarized optical microscope between crossed polarizers) of the morphologies obtained by exploiting the optical setup in Figure 19; (A–C) polar POLICRYPS optical structures with different numbers of rings and pitches; (D) circular POLICRYPS structures obtained by slightly misaligning the setup in Figure 19; (E) magnification of the central area of the structure.
Reprinted with permission from Ref. [39], Optical Society of America (with full citation in reference list).

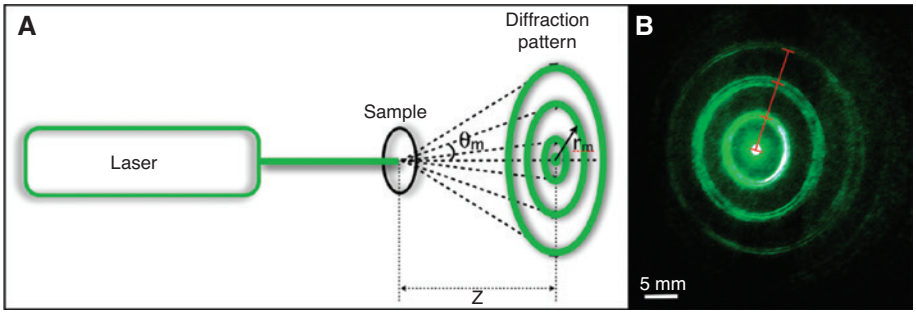

Figure 21: (A) Sketch depicting the diffraction pattern produced by a circular diffraction grating when illuminated with coherent light; (B) picture of the real diffraction pattern produced by the circular POLICRYPS optical diffraction grating when probed with the green laser light. It can be observed that the light intensity of the diffracted orders decreases by increasing the number of the order. However, as a difference from the Cartesian case, measuring the diffraction efficiency of a given order is now more difficult, the light being diffracted in a ring and no more in a point. An estimate of the first-order diffraction efficiency (performed using geometric considerations) gave a value of about 20%.
Reprinted with permission from Ref. [39], Optical Society of America (with full citation in reference list).

the circles of the structure. Where the optical properties of our samples are concerned, they produce a far-field diffraction pattern given by a series of concentric circles: at a distance z from the sample (Figure 21A), the radius r_m of the m-th diffraction ring can be calculated by means of the Bragg theory. Figure 21B shows the circular diffraction pattern produced by the sample with $\Lambda_c \approx 5\ \mu m$, when it is acted on, at normal incidence, by a green laser probe (low power, solid state laser).

8 Conclusions

In conclusion to this review, we have the belief that, in the field of electrically switchable optical devices exploiting liquid crystalline composite materials, the POLICRYPS structure is very promising for several kinds of application. Both 'single-step' and 'multi-step' processes enable fabrication of a rigid, stable, and sharp polymeric frame of 'channels', which can be filled with uniform films of different kinds of LC; all optical applications are based on this distinctive characteristics. As a matter of fact, sharpness of the structure and uniformity of the LC films allow to minimize light scattering losses, while a suitable application of an electric field by means of an external voltage determines a reorientation of the LC director that is exploited to obtain a spatial modulation of the refractive index of the sample. Possible applications in optical technologies depend on the way a light beam propagates through the POLICRYPS while undergoing this modulation. For light impinging at a given angle with the surface of the sample, a POLICRYPS structure, realized with a single-step fabrication process and filled with NLC, has its main application as a switchable diffraction grating, a

beam splitter, a switchable optical phase modulator (if the light beam impinges almost perpendicularly), or a tunable Bragg filter for a light beam impinging parallel to the structure and perpendicular to the channels. A multi-step fabrication process enables the realization of a POLICRYPS-based soft matter template, to align different kinds of liquid crystalline materials or to create an array of tunable microlasers (if filled with a mixture of dye-doped CLC and the system is optically pumped). Finally, a new fabrication setup enables to realize POLICRYPS with a polar symmetry, a structure that opens the possibility to be designed to operate as a q-plate. The performances exhibited in all the above optical devices are very interesting and stimulate further investigations in the different fields.

Acknowledgments: We acknowledge the cooperation of all co-authors of the papers we published on the argument Sameh Ferjani, Alessandro Tedesco, Ivan Trebisacce, V. Barna, N. Scaramuzza from our department; Giovanni Gilardi, Rita Asquini, Antonio d'Alessandro, from Dipartimento di Ingegneria dell'Informazione, Elettronica e Telecomunicazioni, Sapienza Università di Roma; Domenico Donisi, Romeo Beccherelli, from Istituto per la Microelettronica e Microsistemi (CNR-IMM), Roma; Sathyanarayana Paladugu, from Department of Physics, Bilkent University, Ankara, Giovanni Volpe, Domenico Alj, from Soft Matter Lab, University of Gothenburg.

The research leading to these results received partial funding from the European Union's Seven Framework Programme (FP7/2007-2013) under grant agreement no. 228455.

Author contributions

R.C., L.D.S., A.D.L., G.S., N.T., R.B., and C.U. conceived and planned the experiments and contributed to the interpretation of the results; R.C., L.D.S., A.D.L., and S.S. contributed to the preparation of the samples and carried out the measurements; A.V. planned and carried out the simulations; G.S., R.B., and C.U. supervised the research; C.U. took the lead in writing the manuscript. All the authors provided critical feedback and helped shape the research, analysis, and manuscript.

References

[1] R. L. Sutherland, V. P. Tondiglia, L. V. Natarajan, T. J. Bunning and W. W. Adams, J. Nonlinear Opt. Phys. Mater. 5, 89 (1996).
[2] T. J. Bunning, L. V. Natarajan, V. P. Tondiglia and R. L. Sutherland, Ann. Rev. Mater. Sci. 30, 83 (2000).
[3] L. De Sio, R. Caputo, A. De Luca, A. Veltri and C. Umeton, Appl. Opt. 45, 3721 (2006).
[4] R. Caputo, L. De Sio, A. V. Sukhov, A. Veltri and C. Umeton, Opt. Lett. 29, 1261 (2004).
[5] R. Caputo, A. V. Sukhov, C. Umeton and R. F. Ushakov, J. Exp. Theor. Phys. 91, 1190–1197 (2000).
[6] L. De Sio, S. Ferjani, G. Strangi, C. Umeton and R. Bartolino, Soft Matter 7, 3739 (2011).
[7] R. Caputo, A. Veltri, C. Umeton and A. V. Sukhov, J. Opt. Soc. Am. B 21, 1939 (2004).
[8] H. Kogelnik, Bell Syst. Technol. J. 48, 2909 (1969).
[9] Beam Engineering for Advanced Measurements Co., http://www.beamco.com.
[10] U. A. Hrozyk, S. V. Serak, N. V. Tabiryan, L. Hoke, D. M. Steeves, et al., Mol. Cryst. Liq. Cryst. 489, 257 (2008).
[11] U. Hrozhyk, S. Serak, N. Tabiryan, D. Steeves, L. Hoke, et al., Proc. SPIE, 7414, 1 (2009).
[12] L. De Sio, A. Veltri, C. Umeton, S. Serak and N. Tabirian, Appl. Phys. Lett. 93, 181115 (2008).
[13] L. De Sio, S. Serak, N. Tabiryan, S. Ferjani, A. Veltri, et al., Adv. Mater. 22, 2316 (2010).
[14] L. De Sio, N. Tabiryan, R. Caputo, A. Veltri and C. Umeton, Opt. Express, 16, 7619 (2008).
[15] F. Simoni, Nonlinear Optical Properties of Liquid Crystals (World Scientific, New York, 1997).
[16] R. C. Jones, J. Opt. Soc. Am. 31, 488 (1941).
[17] R. Caputo, I. Trebisacce, L. De Sio and C. Umeton, Opt. Express 18, 5776 (2010).
[18] L. De Sio, A. Tedesco, N. Tabiryan and C. Umeton, Appl. Phys. Lett. 97, 183507 (2010).
[19] A. Yariv, Quantum Electronics (J. Wiley, New York, 1989).
[20] A. d'Alessandro, D. Donisi, L. De Sio, R. Beccherelli, R. Asquini, et al., Opt. Express 16, 9254 (2008).
[21] G. Gilardi, L. De Sio, R. Beccherelli, R. Asquini, A. d'Alessandro, et al., Opt. Lett. 36, 4755 (2011).
[22] J. Zou, F. Zhao and R.T. Chen, Appl. Opt. 41, 7620 (2002).
[23] P.G. De Gennes and J. Prost, The Physics of Liquid Crystals, 2nd Ed. (Oxford University Press, United Kingdom, 1995).
[24] R. B. Meyer, Phys. Rev. Lett. 22, 918 (1969).
[25] J. S. Patel and R. B. Meyer, Phys. Rev. Lett. 58, 1538 (1987).
[26] G. Carbone, P. Salter, S. J. Elston, P. Raynes, L. De Sio, et al., Appl. Phys. Lett. 95, 011102 (2009).
[27] T. K. Gaylord and M. G. Moharam, Appl. Opt. 20, 3271 (1981).
[28] G. Hegde and L. Komitov, Appl. Phys. Lett. 96, 113503 (2010).
[29] R. B. Meyer, Mol. Cryst. Liq. Cryst. 40, 33 (1977).
[30] N. A. Clark and S. T. Lagerwall, Appl. Phys. Lett. 36, 899 (1980).
[31] P. Watson, P. J. Bos and J. Pirs, Phys. Rev. E 56, R3769 (1997).
[32] J. B. Lee, R. A. Pelcovits and R. B. Meyer, Phys. Rev. E 75, 051701 (2007).
[33] H. Kogelnik and C. V. Shank, Appl. Phys. Lett. 18, 152 (1971) and references therein.
[34] A. F. Muñoz, P. Palffy-Muhoray and B. Taheri, Opt. Lett. 26, 11 (2001).
[35] G. Strangi, V. Barna, R. Caputo, A. De Luca, C. Versace, et al., Phys. Rev. Lett. 94, 063903 (2005).
[36] M. Ozaki, M. Kasano, D. Ganzke, W. Haase and K. Yoshino, Adv. Mater. 14, 306 (2002).
[37] L. M. Blinov and V. G. Chigrinov, Electrooptic Effects in Liquid Crystal Materials (Springer, New York, 1994).
[38] L. Marrucci, C. Manzo and D. Paparo, Phys. Rev. Lett. 96, 163905 (2006).
[39] D. Alj, R. Caputo and C. Umeton, Opt. Lett. 39, 6201 (2014).

Roberto Caputo
CNR-Nanotec, UOS Cosenza, Dipartimento di Fisica, Università della Calabria, Cubo 31C, Ponte Pietro Bucci, 87036 Rende, Italy

Roberto Caputo obtained his MSc in Physics from the University of Calabria in 2000. In the same year, he received a post-graduate scholarship from INFM (National Institute for the Physics of Matter) for continuing his master thesis research. In 2002, he started his PhD in Physics. In 2005, he obtained a Marie Curie Post-Doc Fellowship for the 'Transfer of Knowledge' at Philips Research Laboratories in Eindhoven, The Netherlands, under the supervision of Dr. Hugo Cornelissen. During the stay at Philips, his research work was mainly focused on the realization of the new concept LCD backlight systems. In 2007, he obtained a 2-year Marie Curie reintegration grant with a project on research and development of highly efficient organic lasing structures. In the same year, he obtained a position as Assistant Professor at the University of Calabria, and he actually is a member of CNR-NANOTEC and the Physics Department of the University of Calabria. His scientific activity is mainly oriented to the study and realization of micro- and nano-scale functional systems in organic composite materials. The results of this research span from fundamental physics advances to innovative high-tech applications. Recently, he spent a 2-year period at the University of Technology of Troyes to perform advanced studies on Active Plasmonics. He has authored and co-authored more than 70 papers on international journals, four international patents, and about 40 communications to scientific conferences and symposia. Moreover, he co-chaired the European COST Action IC1208 'Integrating devices and materials: a challenge for new instrumentation in ICT'. During his career, he supervised more than 15 Master thesis students and three PhD fellows.

Antonio De Luca
CNR-Nanotec, UOS Cosenza, Dipartimento di Fisica, Università della Calabria, Cubo 31C, Ponte Pietro Bucci, 87036 Rende, Italy

Antonio De Luca is an Associate Professor at the University of Calabria, since 2014. In 2009/2010 he was a CNR-IPCF researcher. In 2007, he was the Senior Post Doc at Case Western Reserve University (USA), where he passed a second research period (2012–2014) as Senior Research Associate. He has high experience in optical setups, spectroscopic pump-probe systems, ellipsometry, near-field microscopy, as well as simulation codes. His main areas of interest are molecular reorientation effects in liquid crystals, characterization of spatial solitons in liquid crystals, organic lasers in confined structures, random lasers in soft materials, SNOM nanotomography in soft materials, loss compensation in metamaterial, dielectric singularities in hyperbolic metamaterial gain-loss control, and thermoplasmonic effects at the nanoscale. Antonio De Luca is a co-author of more than 90 scientific publications in international journals, with an H-index of 21 and more than 1800 citations. He was the PI of a 3-year, funded PRIN 2102 national project, titled: 'Plasmon-gain coupling in metal-dielectric nanostructures: compensation of losses towards laser action' (2014–2017) and the key personnel of a European project funded under the 7th Framework Program – FP7-NMP-2008-SMALL-2, titled: 'METACHEM – Nanochemistry and self-assembly routes to metamaterials for visible light' (2009–2103).

Giuseppe Strangi
Department of Physics, Case Western Reserve University, Cleveland, OH, USA

Giuseppe Strangi (http://physics.case.edu/faculty/giuseppe-strangi/) is a Professor of Physics and Ohio Research Scholar in Surfaces of Advanced Materials at Case Western Reserve University. He leads the Nanoplasm Labs (http://nanoplasm.case.edu) at CWRU Cleveland, and he is a senior scientist of the National Research Council (CNR-Italy). Strangi is the President of the Scientific Committee of the Foundation 'Con il Cuore', a national foundation that supports cancer research in Europe, and he is the General Chair of the International Conference – NANOPLASM 'New Frontiers in Plasmonics and Nanophotonics'. Strangi's research interests include condensed matter physics, nano-photonics and plasmonics of electromagnetic materials and cancer nanotechnology. He is a fellow of The Institute of Science of the Origins and of the Case Comprehensive Cancer Center (CWRU), a senior member of the Optical Society of America and American Physical Society.

Roberto Bartolino
CNR-Nanotec, UOS Cosenza, Dipartimento di Fisica, Università della Calabria, Cubo 31C, Ponte Pietro Bucci, 87036 Rende, Italy

Roberto Bartolino Born in Rome on July 26, 1948, Graduate in Physics in Rome in 1972, Doctorat es Sciences Physiques (PhD) Paris XI Orsay in 1982, Full professor of Applied Physics since 1986, Laurea honoris causa in Material and Natural Sciences, University of Bucharest in 2005, On leave to the National Academy dei Lincei in the period 2013–2016, Administrative duties: director of the Physics Department, dean of the science faculty, director of the doctoral school, Advisor in several scientific and technological Italian institutions, Coordinator of the Applied Physics panel for the research national evaluation 2011–2014, Coauthor of about 170 scientific papers in liquid crystals and soft matter physics, H factor 32, citation numbers > 3200.

Cesare Umeton
CNR-Nanotec, UOS Cosenza, Dipartimento di Fisica, Università della Calabria, Cubo 31C, Ponte Pietro Bucci, 87036 Rende, Italy
cesare.umeton@fis.unical.it

Cesare P. Umeton was born in Marsala (Italy) in 1949 and received his Laurea degree in Physics with honors at the University of Pisa

in 1974. He was Assistant Professor, Researcher, and Fixed Term Professor and Associate Professor at the Physics Department of the University of Calabria. Since 2001, he is Full Professor of Experimental Physics at the same department, where he was President of the 'Degree course in Materials Science', and is now coordinator of the 'Optics Group'. He is an OSA fellow, President of the 'Association for Novel Optical Materials and Applications (ANOMA)', member of several national and international scientific associations, member of the organizing committee of several international conferences; he is, and has been, scientific manager of several national and international projects. His research interests are in the field of atomic and molecular physics, magnetic resonance and optics of liquid crystals, and liquid crystalline composite materials. He is co-author of more than 170 articles that appeared in international journals of Physics and Material Science, more than 150 communications at international conferences, and co-author of international patents.

Luciano De Sio
Department of Medico-Surgical Sciences and Biotecnologies, Sapienza Università di Roma, Piazzale Aldo Moro, 5, 00185 Roma RM, Italy

Luciano De Sio is an assistant professor at the Department of Medico-Surgical Sciences and Biotecnologies (Sapienza University of Rome, Italy). He graduated with a Physics degree from the University of Calabria, Italy, in 2003 and did his PhD in Science and Technology of Mesophases and Molecular Materials from the same university in 2006. He was a senior research scientist at the Beam Engineering for Advanced Measurements Company, USA, for almost 5 years (2013–2018). He has extensive experience in the fields of plasmonics, optofluidics, nanomedicine, polymers, optofluidics, and liquid crystals. He has coauthored 90 articles in physics, several book chapters, and 18 international patents and delivered more than 30 scientific communications at conferences. He edited the book 'Active Plasmonic Nanomaterials'. He is also the principal investigator of an international project of the European Office of Aerospace Research and Development (EOARD), supported by the US Air Force Office of Scientific Research (AFOSR) and the Materials and Manufacturing Directorate of the US Air Force Research Laboratory (AFRL).

Alessandro Veltri
Colegio de Ciencias e Ingeniera, Universidad San Francisco de Quito, Quito, Ecuador

Alessandro Veltri received his PhD in Physics in 2005 and has currently a Full Professor position at the Department of Physics of the Universidad de San Francisco de Quito in Quito, Ecuador. During the last 15 years, Dr. Veltri published several scientific papers in peer-reviewed journals and presented his work in many international conferences. His research interests include wave propagation, nonlinear optics, liquid crystals, random systems, photochemistry in composite materials, all optical materials, metamaterials, and hybrid plasmonics. Dr. Veltri worked as a post-doc researcher for the University of Calabria in Italy, the University of Bordeaux, and the Centre de Researche Paul Pascal in France. He was also a visiting researcher at the Case Western Reserve University in Cleveland, Ohio. He is a theorist who used to work side by side with experimentalists, a Linux expert with extensive experience in coding (C, C++, Fortran 77/90/9 5, and Python), and he is trained in high-performance parallel computing and code optimization.

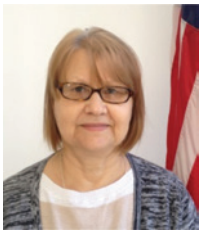

Svetlana Serak
Beam Engineering for Advanced Measurements Company, Orlando, FL, USA

Svetlana Serak is a Senior Optical Engineer at Beam Engineering for Advanced Measurements Corporation. She received a PhD degree in Physics, with specialization on Physical and Quantum Electronics from the Institute of Electronics of the Belarussian Academy of Sciences (Minsk, 1986), where she had a position of the Head of Nonlinear Optics Group. Her group was the first to demonstrate trans-cis isomerization induced with nanosecond laser pulses in azobenzene liquid crystals (1979). Her experience and interests relate to laser physics and engineering, optics, electro-and nonlinear optics of liquid crystals, dynamic holography and phase conjugation, beam combining and beam steering, optical switching and information recording, diffractive waveplates, including gratings and lenses. She has over 100 publications, book chapters, and a series of patents.

Nelson Tabiryan
Beam Engineering for Advanced Measurements Company, Orlando, FL, USA

Nelson Tabiryan is the CEO of Beam Engineering for Advanced Measurements Corporation. He received his PhD degree in Physics and Mathematics from the Institute of Physical Investigations of the Armenian Academy of Sciences, Yerevan, in 1982 and his DSc degree from the Highest Qualifying Commission of the USSR in 1986. He is an OSA fellow and a recipient of the Frederiks Medal. He is the Chairman of Optics of Liquid Crystals (OLC) advisory board (2007–2011); Chairman and co-chairman of international meetings OLC-2005 (Sand Key, Florida), OLC-2007 (Puebla, Mexico), SPIE's Display Sciences (Berlin, Germany, 1996). He is an Alexander von Humboldt Stipendium (1992–1994) recipient and a keynote, plenary, and invited speaker in many major conferences. He has over 250 refereed publications, a monograph, and was a guest editor for conference proceedings. His interests and expertise include diffractive waveplates; optics, electro-optics, and nonlinear optics of liquid crystals; polarization holography; displays; control and characterization of laser beams.